Staphylococcus aureus colonizing the skin microbiota of adults with severe atopic dermatitis exhibits genomic diversity and convergence in biofilm traits

Francesca Sivori [a], Ilaria Cavallo [a], Mauro Truglio [a], Flavio De Maio [b], Maurizio Sanguinetti [b], Giorgia Fabrizio [c], Valerio Licursi [d], Massimo Francalancia [a], Fulvia Fraticelli [a], Ilenia La Greca [a], Federica Lucantoni [c], Emanuela Camera [e], Maria Mariano [f], Fiorentina Ascenzioni [c], Antonio Cristaudo [f], Fulvia Pimpinelli [a], Enea Gino Di Domenico [a,*]

[a] *Microbiology and Virology Unit, San Gallicano Dermatological Institute, IRCCS, Rome, Italy*
[b] *Dipartimento di Scienze di Laboratorio e Infettivologiche, Fondazione Policlinico Universitario "A. Gemelli" IRCSS, Rome, Italy*
[c] *Department of Biology and Biotechnology "C. Darwin" Sapienza University of Rome, Rome, Italy*
[d] *Institute of Molecular Biology and Pathology, National Research Council of Italy, Rome, Italy*
[e] *Laboratory of Cutaneous Physiopathology and Integrated Center of Metabolomics Research, San Gallicano Dermatological Institute, IRCCS, Rome, Italy*
[f] *Clinical Dermatology, San Gallicano Dermatological Institute, IRCCS, Rome, Italy*

ARTICLE INFO

ABSTRACT

Atopic dermatitis (AD) is a chronic inflammatory skin disorder exacerbated by *Staphylococcus aureus* colonization. The specific factors that drive *S. aureus* overgrowth and persistence in AD remain poorly understood. This study analyzed skin barrier functions and microbiome diversity in lesional (LE) and non-lesional (NL) forearm sites of individuals with severe AD compared to healthy control subjects (HS). Notable differences were found in transepidermal water loss, stratum corneum hydration, and microbiome composition. *Cutibacterium* was more prevalent in HS, while *S. aureus* and *S. lugdunensis* were predominantly found in AD LE skin. The results highlighted that microbial balance depends on inter-species competition. Specifically, network analysis at the genus level demonstrated that overall bacterial correlations were higher in HS, indicating a more stable microbial community. Notably, network analysis at the species level revealed that *S. aureus* engaged in competitive interactions in NL and LE but not in HS. Whole-genome sequencing (WGS) showed considerable genetic diversity among *S. aureus* strains from AD. Despite this variability, the isolates exhibited convergence in key phenotypic traits such as adhesion and biofilm formation, which are crucial for microbial persistence. These common phenotypes suggest an adaptive evolution, driven by competition in the AD skin microenvironment, of *S. aureus* and underscoring the interplay between genetic diversity and phenotypic convergence in microbial adaptation.

1. Introduction

Atopic Dermatitis (AD), a common inflammatory skin disorder, poses significant challenges due to its chronic nature and symptom severity. AD is marked by severe pruritus, erythema, and skin barrier dysfunction, among other signs [1]. There is growing evidence that the skin microbiome plays an essential role in the pathophysiology of AD, with *Staphylococcus aureus* recognized as a critical species in this context [2–4].

Staphylococcus aureus is associated with skin health and various skin disorders [5]. In AD, it colonizes the skin and contributes significantly to disease exacerbation [6]. While the host's genetic risk factors are integral to the onset of AD, *S. aureus* colonization and its subsequent interactions with the host immune system often worsen the disease severity [7,8]. The overabundance of this bacterium contributes to immune dysfunction, reduced antimicrobial peptides, heightened allergic reactions, and skin barrier disruption [9]. In addition to dysbiosis, other ecological factors like humidity, temperature, pH, and lipid content influence the regulation of the skin microbiome. In people with AD, the skin exhibits several physiological changes, including increased

transepidermal water loss (TEWL), alterations in the hydration of the stratum corneum (SC), and modifications in the lipidome composition of SC [10,11]. These factors likely influence the skin microbiome's structure and function, resulting in dysbiosis - a phenomenon frequently associated with AD [2]. Intriguingly, *S. aureus* strains show a significant ability to persist in the skin of people with AD. In particular, the dominance of biofilm-growing *S. aureus* in AD lesions is directly correlated with disease severity, thus contributing to sweat duct occlusion, skin inflammation, and pruritus [12,13]. Biofilm formation by *S. aureus* is a complex process mediated by various factors. The adhesion of *S. aureus* to the skin is facilitated by host factors such as fibrinogen, fibronectin, and collagen, which interact with microbial surface components recognizing adhesive matrix molecules (MSCRAMMs). The maturation of biofilms requires the production of an extracellular polymeric matrix composed of host factors, polysaccharide intercellular adhesin (PIA), proteins, extracellular DNA (eDNA), and lipids. The biofilm matrix protects bacteria from host immune responses and antimicrobial agents, challenging eradication [6,14,15].

Distinct sequence types of *S. aureus*, each with unique virulence characteristics and antibiotic resistance profiles, have been associated with specific disease contexts, such as hospital-acquired or community-associated infections [16]. These sequence types represent a rich microbial diversity and complexity, potentially contributing to the pathogen's adaptive evolution and persistence during AD treatment [17,18]. However, despite considerable research efforts and the critical role of *S. aureus* in exacerbating the severity of AD, no specific sequence types have been definitively and robustly linked with this skin condition [19].

Exploring the factors enabling *S. aureus* persistence on AD skin is crucial in understanding the disease's pathophysiology and designing effective prevention and treatment strategies. This study investigated the detailed analysis of the skin physiology parameters and the variations in the skin microbiome associated with *S. aureus* colonization in AD. From this, we evidenced the genetic and phenotypic traits that potentially aid in the adaptation and persistence of *S. aureus* in the AD microenvironment.

2. Materials and methods

2.1. Study design and participant enrolment

Dermatologists collected microbiome samples from the forearm skin of adult subjects (>18 years of age) of unaffected (NL) and lesional (LE) areas of 16 people with AD and 14 healthy subjects (HS) during routine examinations at a single institution. The swabbed area was approximately five cm^2, and 20 streaks were applied during sampling to ensure comprehensive collection. The swabs were pre-moistened with 1x PBS to optimize the recovery of microbial samples. Informed consent was obtained from all subjects and their guardians, ensuring ethical compliance. The Eczema Area and Severity Index (EASI) Score, ranging from 0 (clear) to 72 (very severe), assessed AD severity. Participants with EASI scores between 24 and 58 (mean: 33.5) were classified as AD cases. HS without skin inflammatory conditions or recent skin treatment history were included. The study, conducted from September 2021 to January 2022 at the San Gallicano Dermatological Institute, matched control subjects by age, gender, and skin sampling area to people with AD [20]. Exclusion criteria included recent use of topical treatments. Ethical approval was secured from the Central Ethics Committee I.R.C·C. S. Lazio, Rome (Protocol 641–09.06.2021, trial registry number 1538/21), adhering to the Helsinki Declaration.

2.2. Measurements of epidermal biophysical properties

Dermatologists measured the forearm region of 14 HS and the NL and LE area of 16 people with AD. The study room was maintained at 20–23 °C, 40%–60 % humidity. Participants were required to acclimate to the environment for 15 min and were not allowed to wash or apply emollients at the lesion for 6 h before measurements. Non-invasive instrumental evaluation of skin barrier biophysical parameters was performed by a Tewameter™ 300® (CK Courage Khazaka Electronic, Köln, Germany), which was used to calculate the water evaporation rate in g/h/m2 and a Corneometer CM 820 (CK Electronic, Köln, Germany), which was used to assess the water content in the stratum corneum (arbitrary units) [20].

2.3. Strain identification and collection

Sterile Copan swabs (Copan, Brescia, Italy) collected samples from the forearm region of the LE of 16 people with AD. Swab suspensions were cultured on Columbia CNA agar with 5 % sheep blood (Becton Dickinson, Heidelberg, Germany) and blood agar (Oxoid, Milan, Italy). The initial bacterial identification was performed by the MALDI-TOF MS system (Bruker Daltonik, Bremen, Germany). For the detected *S. aureus*, at least seven phenotypically identical colonies were isolated and stored at −80 °C. DNA extraction followed for each colony, with the 16S rRNA gene sequence confirming species [21]. Genetic diversity among *S. aureus* from skin samples was assessed via random amplified polymorphic DNA polymerase chain reaction (RAPD-PCR) analysis, setting an 80 % similarity threshold for clonal grouping [22]. The prevalent clonal group (detected in 85–100 % of colonies) was identified as the dominant type. A representative isolate of each dominant clonal group was selected for further analysis.

2.4. Sequencing and analysis

From the skin samples of the study participants, extracted DNA was amplified by PCR with dual-index primers targeting the V1–V3 regions of the bacterial 16S rRNA gene, using the ARROW for NGS Microbiota solution A kit (ARROW Diagnostics) according to the manufacturer's instructions. A sterile sample tube that had undergone the same DNA extraction and PCR amplification procedures was used for quality control. Before sequencing, amplicons were purified using the Agencourt® AMPure XP PCR purification system (Beckman Coulter, Milan, Italy), and equal amounts (10 nM) of the sample's DNA were pooled and diluted to reach a 4-nM concentration. Finally, 5 pM of the denatured libraries was used to generate sequences using the 2 × 250 cycles MiSeq Reagent kit (Illumina) on an Illumina MiSeq instrument. Sequencing data were analyzed using the MicrobAT system [23]. During MicrobAT processing, demultiplexed sequences showing reads of length less than 200 nucleotides, an average Phred quality score below 25, and at least one ambiguous base was discarded. The resulting sequences were aligned at a 97 % sequence similarity and assigned to taxonomic (e.g., species) levels at an 80 % classification threshold using the Ribosomal Database Project (RDP) classifier (release 11.5). Species not meeting these criteria were assigned to the corresponding group, "unclassified [genus]". The Biological Observation Matrix (BIOM) was obtained, and the following analysis was carried out in R studio (https://www.rstudio.com/;version 4.0.2) using the phyloseq package. Microbial community differences were measured for alpha and beta diversity after reading depth rarefaction. Shannon index and Pielou index were used to evaluate alpha diversity, and the Kruskal Wallis test assessed significance. Bray Curtis beta diversity was calculated, and the distance matrix was represented as Principal coordinate analysis (PCoA). Significance was evaluated by Permutational multivariate analysis of variance (PERMANOVA). Bacterial relative abundances between selected groups at phylum and genus levels were examined [23].

The linear discriminant analysis Effect Size (LEfSe) tool has been used to identify genera and phyla with the highest abundance in HS, NL, and LE skin microbiomes [24].

2.5. Co-occurrence/co-exclusion relationships network analysis

Correlation networks were generated for HS, NL, and LE. Initial

filtering removed OTUs with fewer than 2000 reads across samples or below 4000 for combined time point analysis, representing <0.05 % average relative abundance. OTUs with zero counts were subsequently excluded in each time-specific analysis. Spearman's rank correlation coefficients, using R version 4.3.1, assessed the correlation among OTUs favored for non-normally distributed data [25]. The *qgraph* package (version 1.9.5) in R visualized the networks, applying a 0.4 (or 0.5 for bacteria and fungi) correlation coefficient threshold to filter out minor relationships. Edge width and color saturation were scaled with a 0.5 threshold for both correlations. Differences in Spearman's correlation distributions across time points were evaluated using Wilcoxon tests.

2.6. Whole-genome analysis

Fifteen *S. aureus* isolates were collected from the lesional skin of the sixteen people with AD and subjected to whole-genome analysis (WGS). According to the manufacturer's protocols, DNA was extracted for WGS using QIAsymphony DSP Virus/Pathogen Kits (Qiagen, Hilden, Germany). Quality DNA reads were trimmed with FastP v0.23.4 and assembled using SPAdes v3.15.5 [26,27]. The assembled sequences were annotated with Prokka v1.14.6. The pan-genome analysis employed Roary v3.13.0 [28]. Antibiotic resistance gene predictions were made using the Comprehensive Antibiotic Resistance Database (CARD) v3.2.8 and the Resistance Gene Identifier (RGI) tool, focusing on "perfect" and "strict" matches against high-quality reference sequences with a 97 % identity cutoff for inclusion [29]. Virulence factors (VF) were identified using Blastn against the Virulence Factor Database (VFDB), considering hits with ≥80 % coverage and ≥90 % identity [30].

2.7. Antibiotic susceptibility

The antimicrobial susceptibility was assessed by the BD PhoenixTM automated microbiology system (Becton Dickinson Diagnostic Systems, Maryland, USA) and by the broth microdilution test (Thermo Scientific, Massachusetts, USA). Results were interpreted to define the Minimum Inhibitory Concentration (MIC) criteria, according to the European Committee on Antimicrobial Susceptibility Testing (EUCAST) clinical breakpoints (http://www.eucast.org/clinical_breakpoints).

2.8. Biofilm formation

Evaluation of biofilm formation was quantified using crystal violet (CV) to assess biomass 24 h post-incubation. Sterile 96-well polystyrene plates were inoculated with 200 µl of an initial bacterial suspension (10^5 CFU/ml) in CAMHB incubated at 37 °C for 24 h without shaking. Each strain was evaluated in triplicate. The medium was removed from the wells and washed thrice with 200 µl sterile distilled water. The plates were air-dried for 45 min, and the adherent cells were stained with 200 µl of 0.1 % crystal violet solution. After 15 min, the dye was removed, and the wells were washed three times with 200 µl of sterile distilled water to remove excess stain. The dye incorporated by the cells forming biofilm was dissolved with 200 µl of ethanol-acetone, 4:1, and the absorbance of each well was measured spectrophotometrically at 570 nm (OD570) by using the Multiskan SkyHigh (Thermo Fisher Scientific, Ohio, USA) [31]. Viable cell counts were determined through plate counting to measure CFU/ml. Experiments were performed in triplicate and repeated three times. Each plate and assay included *S. aureus* strain ATCC 6538 as standard reference and internal control.

2.9. Bacterial adhesion

Early bacterial adhesion was quantified by the BioFilm Ring Test (BRT) as previously described [23,32], using the reagents and equipment provided by the Biofilm Ring Test® kit (KITC004) and analyzed by the BFC Elements 3.0 software (Biofilm Control, Saint Beauzire, France). Twelve wells containing the BHI/TON mix without microbial cells were included in each experiment as negative controls. Each strain was analyzed in duplicate, and experiments were repeated three times.

2.10. Determination of metabolic activity

The metabolic activity of biofilm isolates was determined using a Phenol red assay as previously described with slight modification [33]. For biofilm formation, after 5 h at 37 °C, the wells were rinsed with 0.45 % saline solution, and 200 µL of a CAMHB/phenol red solution at 25 µg/ml concentration was added. The plate was incubated for 20 additional hours at 37 °C, and absorbance (560 nm) was recorded in 20-min periods for 1200 min using a multidetector microplate reader.

2.11. Hemolysis assay

Bacterial colonies, grown overnight on blood agar plates, were inoculated into 2 ml of 0.45 % saline solution to obtain turbidity of 0.5 ± 0.1 McF corresponding to approximately 1×10^8 CFU/ml, diluted 1:100 in CAMHB and incubated overnight at 37 °C. *S. aureus* cells were centrifuged, and the supernatants were used to measure hemolytic activity. 100 µl of supernatants were added to 1 ml of PBS containing 25 µl rabbit red blood cells. The blood cells and *S. aureus* were incubated at 37 °C for 60 min to determine hemolytic activities. Supernatants were collected by centrifugation at 4000*g* for 10 min, and optical densities were measured at 543 nm in a microplate reader (Multiskan SkyHigh; Thermo Fisher Scientific, USA). In addition, the incubation of Triton X-100 and sheep red blood cells was used as the positive control, and the incubation of PBS and sheep red blood cells served as the negative control.

PBS was used as a negative control group. The assays were performed in triplicate, and the percentage of hemolysis value was calculated by comparing it with the positive control (100 % hemolysis) [34].

2.12. Desiccation tolerance

The desiccation tolerance was tested for five days, as described previously, with some modifications [35]. For each experiment, an overnight culture of *S. aureus* grown on a Columbia sheep agar plate was used to inoculate 2 mL of 0.45 % saline solution to 0.5 ± 0.1. For biofilm cultures, diluted cell suspensions (approximately 10^7 CFU/mL) were used to inoculate a 24-well polystyrene flat-bottom plate with 1000 µL CAMHB, preparing one for each period of 1, 2, and 5 days. After 24 h at 37 °C, the well contents were aspirated and then rinsed with 0.45 % saline solution to remove non-adherent bacteria. An empty plate was left at room temperature for each time point. The wells were scraped thoroughly, and the total number of viable cells was determined by serial dilution and plating on Columbia sheep agar plates to estimate the CFU number.

2.13. Enterotoxins

The presence of enterotoxins was confirmed via an agglutination test using the SET-RPLA KIT TOXIN DETECTION KIT (Oxoid, Milan, Italy) and following the manufacturer's instructions [36].

3. Results

The study included 16 subjects with severe AD (ten males, six females) and 14 healthy controls (HS) (Fig. 1a). Table 1 and Supplementary Table 1 present the demographic and clinical data, showing both groups matched for age and biological sex. Stratum corneum (SC) hydration and transepidermal water loss (TEWL) were measured on the forearm to assess skin integrity (Fig. 1b–c). SC hydration was significantly higher (P < 0.001) in HS compared to LE in AD subjects. TEWL was significantly higher in LE compared to NL (P = 0.0007) and HS (P < 0.0001). No significant TEWL difference was found between NL and HS.
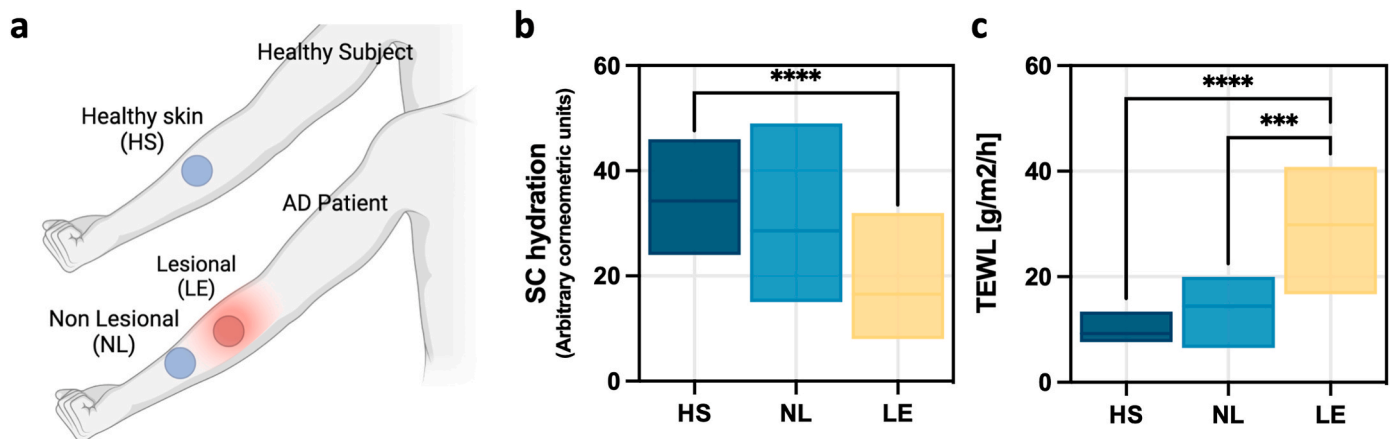
Fig. 1. Sampling procedure in adults with severe AD. **(a)** The study enrolled 14 healthy control subjects and 16 adults with severe AD, determined by the Eczema Area and Severity Index (EASI). Samples were taken from the forearms of healthy control subjects (HS) and the lesional (LE) and non-lesional (NL) sites on the forearms of people with AD. **(b)** Changes in transepidermal water loss rates (TEWL) and C, stratum corneum (SC) hydration levels. Data are expressed as mean ± standard error of the mean. *, P < 0.05; **, P < 0.01; ***, P < 0.001, ****, P < 0.0001; ns, not significant.

Table 1
Demographic and clinical characteristics of people diagnosed with atopic dermatitis (AD) upon enrolment into the study. EASI, Eczema Area and Severity Index (EASI).

Factors	AD cases
Total number	N = 16
Age median (range)	37 years [21–62]
Sex	10 males/6 females
EASI score, median (range)	33.5 [24–58]

These findings indicate skin barrier impairments in AD subjects are mainly restricted to LE, while NL skin resembles HS. Consequently, we analyzed whether the modulation of the skin barrier function affected the bacterial diversity in people with AD and compared it with that of HS.

3.1. Diversity of the skin microbiome

The alpha diversity showed that NL and LE samples had higher Shannon entropy (P = 0.01) and Pielou's evenness (P = 0.04) than HS (Fig. 2a–b). Bray-Curtis beta diversity analysis confirmed distinct spatial clustering for HS samples (P = 0.001), with less defined clusters for NL and LE (Fig. 2c).

Microbiome analysis highlighted a striking dominance of Pseudomonadota across all samples. Actinomycetota was more prevalent in HS (0.29) and less in NL and LE (Supplementary Fig. 1a). At the genus level (Supplementary Fig. 1b), *Cutibacterium* was most abundant in HS (0.31) but decreased in NL (0.06) and LE (0.09). *Staphylococcus* abundance remained stable across NL (0.07), LE (0.18), and HS (0.15).

Linear discriminant analysis (LDA) with effect size (LEfSe) identified significant microbial taxa differences (Fig. 2d). *Propionibacterium* and *Cutibacterium granulosum* were significantly higher in HS. *Sphingomonas*, *Pelomonas*, *Serratia*, *Pseudomonas*, and *Pseudomonas panacis* were more prevalent in NL. *Staphylococcus aureus* and *Staphylococcus lugdunensis* were significantly more abundant in LE.

Network analysis at the genus level (Supplementary Fig. 1c) revealed significantly higher overall, positive, and negative bacterial correlations in HS compared to NL and LE (P < 0.0001). Network analysis at the species level (Fig. 2e), examining *S. aureus* interactions, demonstrated that overall and positive correlations were comparable across HS, NL, and LE. Notably, negative correlations, indicating competitive interactions, were observed only in NL and LE but were absent in HS.

3.2. Whole-genome analysis of Staphylococcus aureus isolates

Network analysis revealed that *S. aureus* engages in competitive interactions in AD environments, which may contribute to its dominance in these conditions, unlike in HS. To explore these findings, we performed a comprehensive genetic and phenotypic analysis to identify the specific adaptations that enable *S. aureus* to persist in the AD microenvironment. As the most prevalent bacteria in LE, *S. aureus* was collected from the lesional skin of individuals with AD and subjected to WGS. To assess genomic conservation across *S. aureus* isolates, the coding sequences were used to determine the pan-genome. The core genome constituted the largest portion of each strain's genome (median, min-max; 83.11 %, 78.40–84.54 %), followed by the accessory genome (median, min-max; 16.26 %, 14.79–17.33 %) and then the unique genome (median, min-max; 1.00 %, 0.00–4.80 %).

As shown in Fig. 3a, the 15 *S. aureus* strains were distributed across different sequence types (STs). The most frequent was ST398 (n = 5; 33.3 %), followed by ST5, ST7, ST22 and ST59 (n = 2; 13.3 % each). Two strains, identified as ST72 and ST106, were present as a single ST (SST). The *S. aureus* strain ATCC 6538 (ATCC strain), used as a reference, was confirmed as ST464 [37]. The Comprehensive Antibiotic Research Database (CARD) identified 21 antimicrobial resistance genes (ARGs) in these strains (Fig. 3b). The most prevalent genes were *arlR*, *kdpD*, *mepR*, *mgrA*, *norC* (100 %), and *lmrS* (93.3 %). Of the 15 screened isolates, two strains (13.3 %) belonging to the ST22 tested positive for *mecA*. Additionally, we determined the prevalence of 52 virulence factor genes, including those for surface attachment (MSCRAMM - microbial surface components recognizing adhesive matrix molecules), biofilm formation, exotoxin and enterotoxin production, and capsule biosynthesis in the *S. aureus* isolates (Fig. 3b).

Overall, 77.8 % of the isolates carried virulence factor genes. Specifically, MSCRAMM genes had a prevalence of 69.0 %, with the clumping factor genes *clfA* and *clfB* found in 73.3 % and 80 % of isolates, respectively. The fibronectin-binding proteins A (*fnbA*) and B (*fnbB*) were present in 86.7 % and 40 % of the strains. The *S. aureus* surface protein C (*sasC*) gene was less common, detected in 33.3 % of isolates. All isolates possessed the biofilm-related *icaABCD* operon genes.

Exotoxin genes were detected in 84.7 % of the isolates, with the toxic shock syndrome toxin (*tsst-1*) gene present in 100 % of AD-associated strains. Panton-Valentine leukocidin genes (*pvlF* and *pvlS*) were detected in 42.8 % of isolates. Enterotoxin genes were the least represented, found in 44.4 % of isolates, with *sea* and *seb* detected in 86.7 % and 46.7 %, respectively. Capsule (*cap*) genes were present in 91.7 % of the isolates, except for *capH* and *capK*, which were found in 33.3 %.
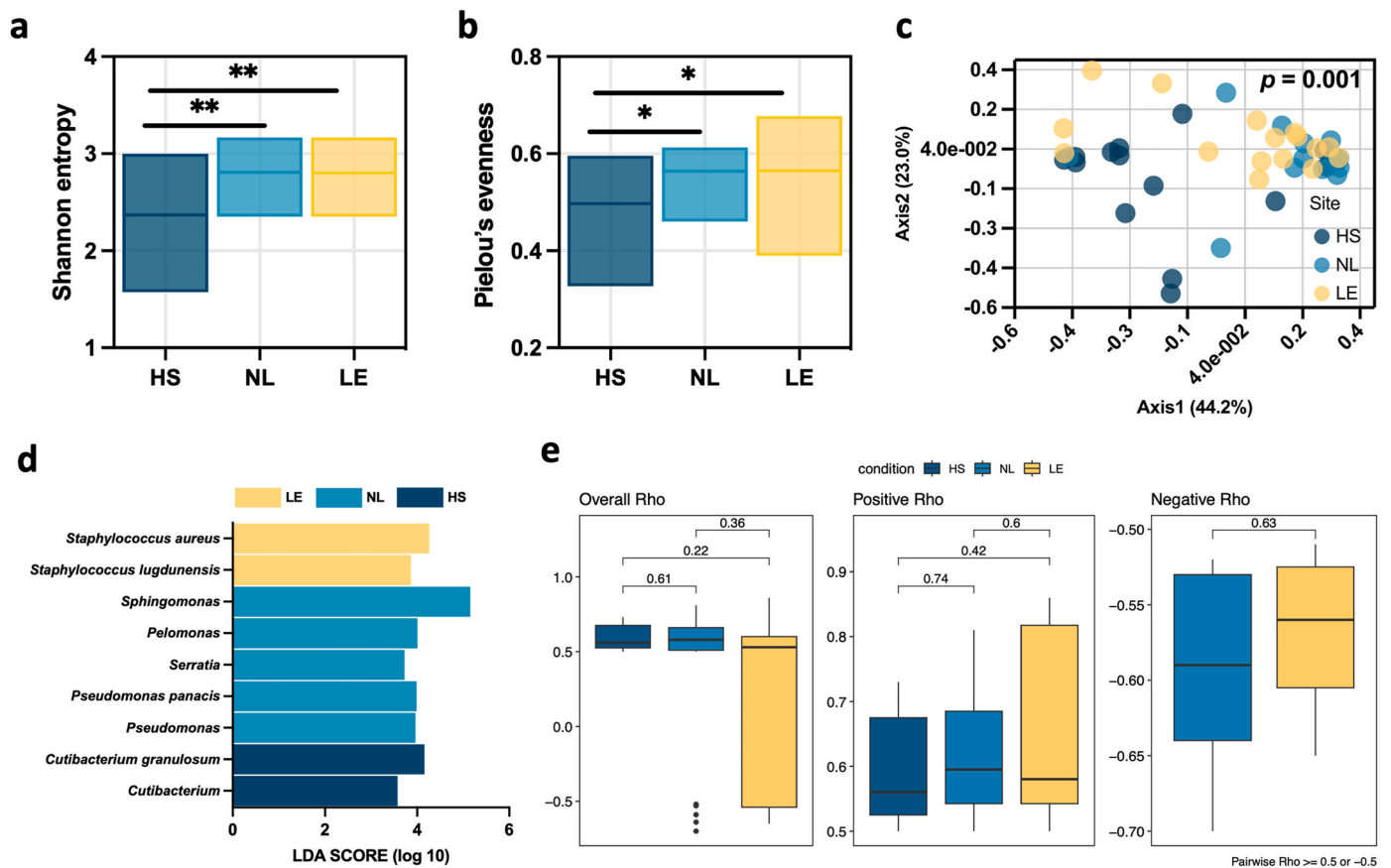
Fig. 2. Alpha and beta diversity, microbiome composition, and network analysis. Alpha diversity was calculated using the **(a)** Shannon entropy and **(b)** Pielou evenness index in healthy control subjects (HS) and the lesional (LE) and non-lesional (NL) sites on the forearm of people with AD. Statistical differences were determined using the Kruskal–Wallis test. **(c)** Bray-Curtis dissimilarity beta diversity was calculated at the genus level and represented as principal coordinate analysis (PCoA). PERMANOVA test was used to assess significance. *, $P < 0.05$; **, $P < 0.01$; ***, $P < 0.001$, ****, $P < 0.0001$. **(d)** Linear discriminant analysis (LDA) combined with effect size (LEfSe) to pinpoint taxonomic distinctions in the skin microbiome between HS, NL, and LE areas, with an LDA threshold score of 3.5. **(e)** *S. aureus* co-occurrence and co-exclusion network attributes at the species level in HS, NL, and LE. Differences in Spearman's r values between HS, NL, and LE (*, $P < 0.05$; **, $P < 0.01$; ***, $P < 0.001$, ****, $P < 0.0001$; ns, not significant) were determined via the Wilcoxon test.
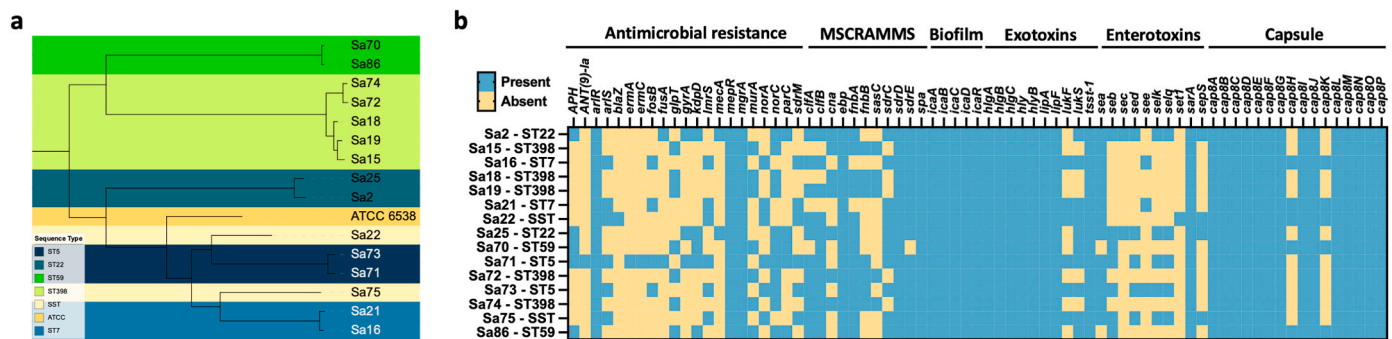

Fig. 3. Whole-genome analysis and functional gene distribution in *S. aureus* isolate. (a) Phylogenetic tree of the 15 *S. aureus* isolates. The *S. aureus* ATCC 6538 strain was also included in the analysis. Branch lengths (-$\log_{10}$ scale) expressed on the tree are proportional to the phylogenetic distances. Different colors were used to highlight the sequence types (ST). **(b)** Distribution of 73 selected factors across different ST categories, indicating the presence (blue) or absence (yellow) of genes in *S. aureus* associated with antimicrobial resistance, surface adhesion (microbial surface components recognizing adhesive matrix molecules - MSCRAMMs), biofilm formation, exotoxin and enterotoxin production, and capsule biosynthesis. (For interpretation of the references to color in this figure legend, the reader is referred to the Web version of this article.)

3.3. Characterization of virulence factors of Staphylococcus aureus clinical isolates

To understand the phenotypic basis of genetic variability, we characterized adherence, biofilm formation, hemolytic activity, desiccation tolerance, and enterotoxin production compared to the reference ATCC strain. No significant differences were observed in early bacterial adhesion capacity among the STs (Fig. 4a). Biomass production varied, with the ATCC strain showing significantly higher production than ST22 ($P < 0.0003$), ST398 ($P = 0.0211$), and SST ($P < 0.0001$) (Fig. 4b). The biofilm matrix of the ATCC strain harbored more cells than ST59 ($P = 0.0079$) and SST ($P = 0.0433$) (Fig. 4c). Metabolic activity within the
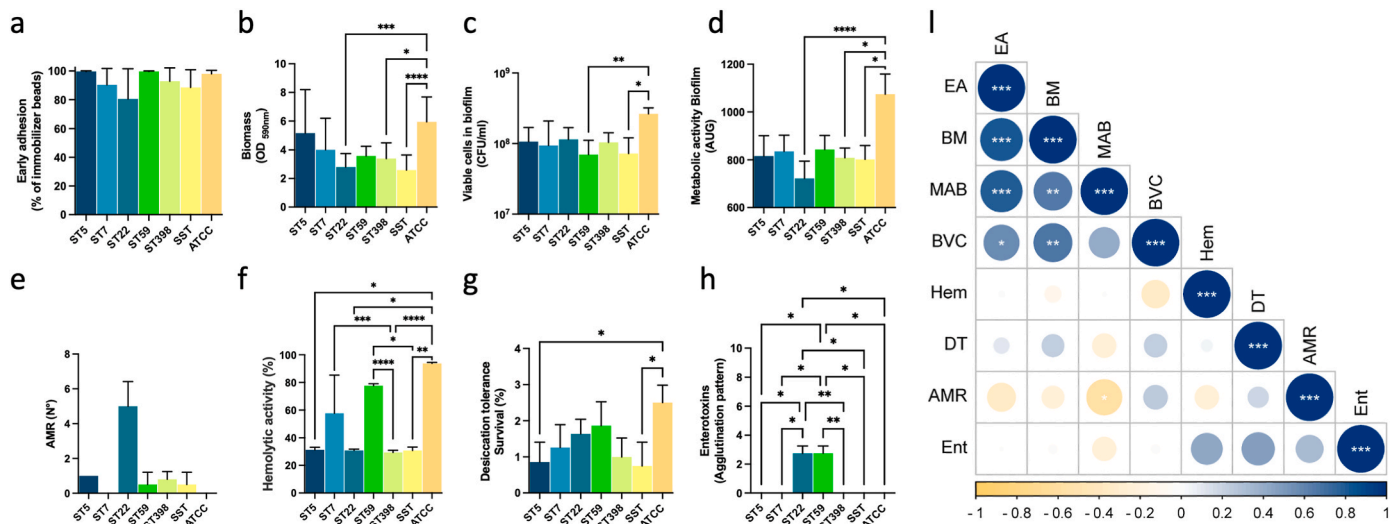
Fig. 4. Phenotypic profiles among the *S. aureus* isolates. Bar plot showing **(a)** early adhesion; **(b)** biomass; **(c)** viable cell count in biofilm; **(d)** metabolic activity in biofilm; **(e)** antimicrobial resistance (AMR) profile; **(f)** hemolytic activity; **(g)** desiccation tolerance after five days; **(h)** agglutination test for enterotoxins. **(i)** Correlation analysis for early adhesion (EA), biomass (BM), biofilm viable cells (BVC), cell metabolic activity in biofilm (MAB), antimicrobial resistance (AMR) profile, hemolytic activity (Hem), desiccation tolerance (DT), enterotoxins production (Ent). Spearman correlation significance indicated by * $P < 0.05$, **$P < 0.01$, ***$P < 0.001$.

biofilm, measured as area under the growth curve (AUG), was significantly higher in the ATCC strain compared to ST22 ($P < 0.0001$), ST398 ($P = 0.0187$), and SST ($P = 0.0382$) (Fig. 4d).

The antimicrobial susceptibility testing (AST) showed that all isolates were susceptible to linezolid, rifampicin, teicoplanin, tigecycline, and vancomycin (Fig. 4e and Supplementary Fig. 2). ST22 shows the highest antimicrobial resistance (AMR) profile, with two strains resistant to oxacillin, confirmed by the presence of the *mecA* gene. The ATCC strain was susceptible to all antibiotics tested.

ST7, ST59, and SST exhibited the greatest hemolytic capacities compared to the other strains (Fig. 4f). The ATCC strain had the most robust desiccation tolerance, a trait associated with environmental persistence and capsule production, significantly greater than ST5 ($P = 0.0456$) and SST ($P = 0.0213$) (Fig. 4g).

Four isolates (26.6 %) were positive for enterotoxins (Fig. 4h). ST22 and ST59 were positive for enterotoxins C and B, respectively. The ST22 strains harbored the *sec* gene, while ST59 strains were positive for the *seb* gene. Although the *seb* gene was also present in ST5, ST22, and SST strains, none were positive for enterotoxin B. Except for ST59, all isolates were positive for the *sea* gene but negative for enterotoxin A.

Given the limited variability, we investigated whether different phenotypes covary, indicating coregulation, or vary independently, suggesting distinct regulatory mechanisms. Correlation analyses showed direct positive correlations ($P < 0.05$) between biofilm-related parameters, including early adhesion, biomass, cell metabolic activity in biofilm, and biofilm viable cells (Fig. 4i).

3.4. Difference between phylogenetic and phenotypic clustering

The phenotypic analysis was used to correlate the genomes of all the isolates. Specifically, a phylogenetic tree was generated based on the distances of the combination of 73 ARG/VF genes and the eight phenotypic factors described in Fig. 4a–h. Phylogenetic analysis within clinical isolates produced distinct clusters corresponding to different STs (Fig. 5a). Interestingly, strains with different genetic backgrounds often exhibited similar virulence-associated phenotypes. To examine the relationship between genomic and phenotypic similarity, the genotype data was normalized and used to cluster the strains based on their phenotypes (Fig. 5b). Notably, the clustering of the phenotypic data was different from the phylogenetic clustering. To compare phenotypic and

phylogenetic clusters, phenotypic data was grouped according to the order of phylogenetic clustering and reported in the heatmap (Fig. 5c). In the heatmap, the lower left section (blue) is colored based on the phylogenetic distance between strains. In contrast, the upper right section (orange) is colored according to the phenotypic distance. The resulting heatmap's lack of symmetry indicated no correlation between phenotypic and phylogenetic distances. To systematically verify this, distances between strains from both data sets were plotted against each other (Fig. 5d). This plot confirmed no correlation between phylogenetic and phenotypic distances ($r = -0.05$).

4. Discussion

The study cohort comprised 16 subjects diagnosed with severe AD, characterized by high EASI scores [38]. This selection, in a subset where AD manifests with heightened clinical and microbiological challenges, facilitated a focused investigation into the disrupted skin barrier and persistent *S. aureus* colonization [19]. Selecting the forearm as the site of study was a deliberate choice. Indeed, the forearm, being an easily accessible area, often exhibits pronounced AD symptoms, making it an ideal site for consistent, non-invasive sampling [39]. Moreover, the forearm's exposure to environmental factors and its involvement in daily activities make it a relevant site for studying AD's impact on skin barrier function and microbial colonization [39,40]. As expected, the study demonstrates compromised skin barrier function in people with AD, as evidenced by altered stratum corneum hydration and increased TEWL compared with HS. This observation aligns with previous findings emphasizing the critical role of barrier dysfunction in the initiation and exacerbation of AD [41–43] and suggesting that the integrity of the skin barrier is inversely related to the severity of AD symptoms [20].

Compared with HS, this study demonstrated a global skin dysbiosis in AD at the forearm. The Shannon entropy and Pielou's evenness increased in diseased subjects, indicating a higher number of bacterial species in individuals with AD than in healthy individuals. This finding contrasts with the previous literature, which reported a lower Shannon diversity in AD than HS, primarily attributed to *S. aureus* [5]. Nevertheless, these variations can be linked to the specific skin site analyzed. Indeed, our data are consistent with findings showing increased Shannon diversity and a higher bacterial richness in AD subjects compared to healthy controls at the forearm [44].
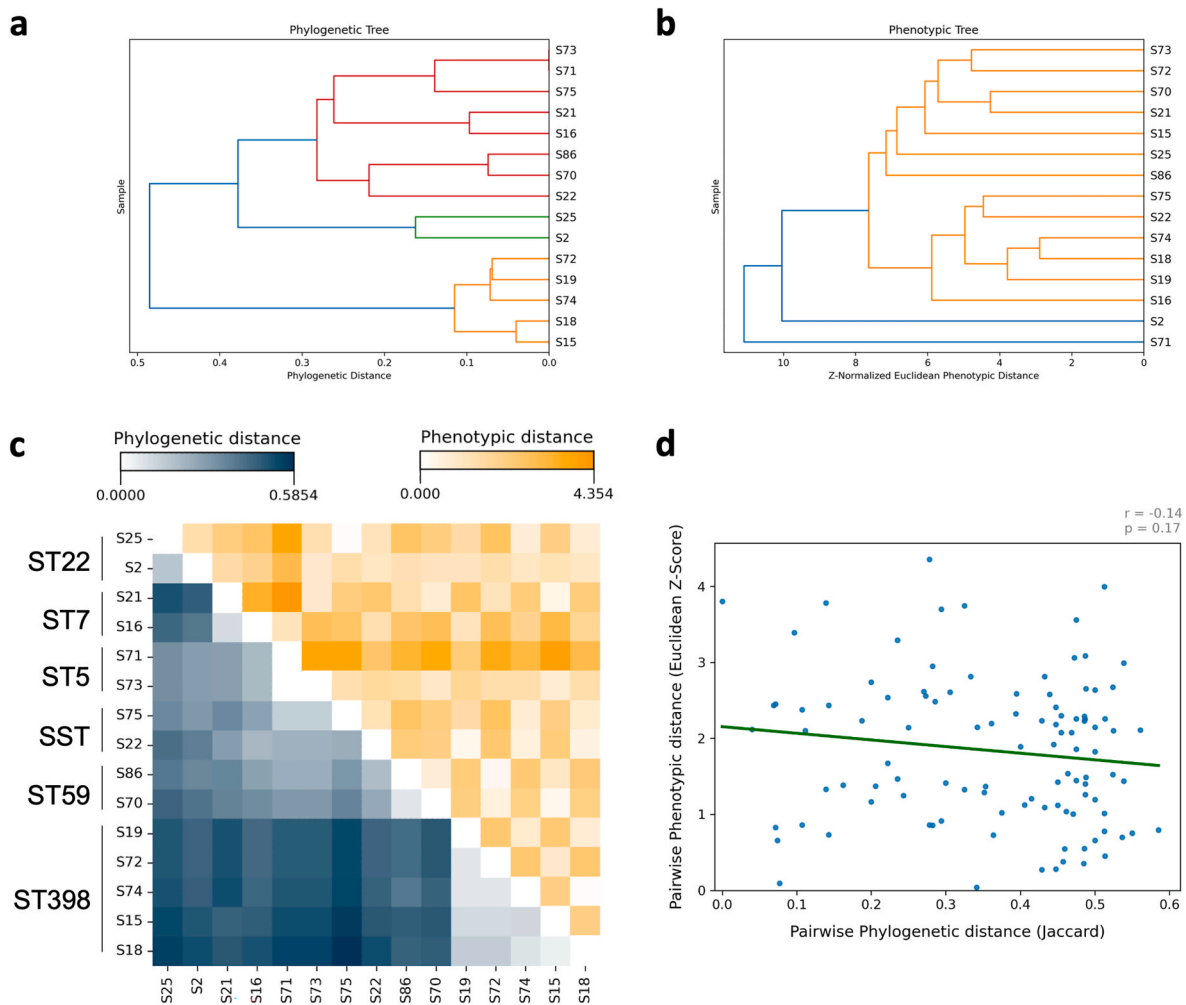
Fig. 5. Correlation of phylogenetic and phenotypic data among *S. aureus* isolates. (a) Phylogenetic tree of the *S. aureus* isolates, based on 73 ARG/VF genes. **(b)** Phenotypic clustering based on the eight phenotypic assays. **(c)** The phenotypic data is reorganized according to the clustering order determined from the phylogenetic tree. White to dark blue color is used to display phylogenetic distance. White to orange color is used to display phenotypic distance. **(d)** Pairwise phylogenetic distance compared with the pairwise phenotypic distances. (For interpretation of the references to color in this figure legend, the reader is referred to the Web version of this article.)

Dry areas like the forearm contain greater bacterial diversity than other human skin sites [45] harboring numerous phylotypes, including Pseudomonadota, Corynebacteria, and Flavobacteriales [46]. LEfSe analysis revealed a higher relative abundance of *Propionibacterium* and *Cutibacterium granulosum* in HS, suggesting a protective role against AD. *Propionibacterium*, known for its anti-inflammatory properties and ability to produce short-chain fatty acids like propionate and acetate, could contribute to maintaining skin pH and suppressing the overgrowth of pathogenic bacteria [47]. *Cutibacterium granulosum*, on the other hand, has been implicated in maintaining skin health through the modulation of skin immunity and the inhibition of pathogen colonization [48]. Specifically, *C. granulosum* is considered to play a pivotal role in sustaining skin health by inhabiting ecological niches, potentially preventing colonization by more pathogenic microorganisms. It produces short-chain fatty acids, thiopeptides, bacteriocins, and other compounds that exhibit inhibitory effects on these harmful organisms [47].

C. granulosum shares numerous traits with *C. acnes*, including the preference for similar habitats [49]. This corroborates the importance of these genera in skin health [49]. In contrast, the increase of *Sphingomonas*, *Pelomonas*, *Serratia*, and *Pseudomonas* genera in the NL skin of people with AD points to a microbial shift that may be associated with disease pathology. *Sphingomonas* is a genus linked with healthy skin and various skin conditions, suggesting its role may be context-dependent

[50,51]. The other genera identified are not typical skin commensals, and their presence could reflect a disrupted skin barrier characteristic of the forearm in AD, allowing these typically environmental or opportunistic pathogens to colonize the skin. Conversely, the prominence of *S. aureus* and *S. lugdunensis* in LE skin could drive inflammation in AD [5, 52]. The role of *S. lugdunensis* in AD's pathogenesis is a subject of ongoing research and debate. *S. lugdunensis* is part of the normal skin flora and is often overshadowed by *S. aureus* [53]. However, recent findings suggest this bacterium may play a more significant role in AD than previously recognized [52]. In AD, where the skin barrier is compromised, the pathogenic potential of *S. lugdunensis* could be augmented, enabling it to contribute to skin inflammation and infection [52]. Increased abundance of *S. aureus*, *S. capitis*, and *S. lugdunensis* in the forearm was positively correlated with increasing AD severity [52].

In our subset of people with AD, *S. aureus* was significantly more abundant, particularly within the LE skin of individuals with AD. This observation is consistent with existing literature that associates *S. aureus* with exacerbated symptoms and increased severity of AD [54]. The preference of *S. aureus* for lesional skin sites is hypothesized to stem from AD's impaired skin barrier and immune dysregulation characteristic, providing a receptive niche for *S. aureus* colonization and proliferation [4]. The network analysis at the genus level provides significant insights into the microbial dynamics within the skin microbiome of individuals

with AD compared to HS [55]. The significantly higher overall bacterial correlations in HS compared to both NL and LE skin of AD subjects highlight the stability of the microbial community in healthy skin. Positive correlations, representing co-occurring bacterial interactions, were markedly lower in both NL and LE than in HS, indicating decreased cooperative interactions within AD-affected skin, likely due to the inflammatory milieu and altered skin barrier function [56,57]. Lastly, negative correlations, indicating competitive interactions among bacteria, were significantly higher in HS than NL and LE, suggesting increased resilience against disturbances in HS [25]. The reduction in competitive interactions might contribute to the instability and dysbiosis observed in the AD microbiome [57] compared to HS [5,6]. In particular, the network analysis, performed at the species level between *S. aureus* and the rest of the bacterial population, revealed that negative correlations were only present in NL and LE but not in HS. This suggests that *S. aureus* engages in competitive interactions with other bacteria in AD-affected skin, likely contributing to its persistence and dominance. The competitive environment in NL and LE may drive the evolution of highly specialized *S. aureus* strains adapted to exploiting the niches created by the disrupted skin barrier and altered immune responses in AD patients [3,25,50].

WGS of 15 *S. aureus* isolates is consistent with findings from other studies identifying a heterogeneous group of STs in people with AD [22]. The most common ST was ST398, associated with zoonotic transmission [58]. Its presence in AD could indicate a broader host range and environmental reservoir for this strain than previously thought. In a recent article, ST398 was also isolated from the skin of people with AD but not from healthy individuals [22]. This observation challenges the established understanding of ST398 as primarily a livestock-associated strain. ST5, ST7, ST22, and ST59 are recognized for their roles in hospital and community-acquired infections due to a virulence profile that poses a risk for transmission within healthcare settings [59–62]. In addition, the prevalence of sequence types ST5, ST7, ST22, and ST59 among people with severe AD may indeed be supported by their frequent and prolonged exposure to hospital environments due to the nature of their condition. Prolonged hospital visits and interventions can increase the risk of colonization by these strains, thereby contributing to the observed ST heterogeneity in this group of people with AD. These STs underscore the complex etiology of AD, where bacterial genetics overlap with host and environmental factors.

The phenotypic profiles of *S. aureus* isolates demonstrate a range of virulence factors yet show distinct divergence from the ATCC strain. Despite displaying lower efficiency than the ATCC strain, all isolates were strong biofilm producers according to conventional classification [63]. The isolates' ability to form robust biofilms can contribute to their persistence on the skin and resistance to antimicrobial treatments, which are critical factors in the pathogenesis and chronicity of AD. The ubiquitous presence of the *ica* operon across all isolates reinforces the role of biofilm formation in *S. aureus* persistence and resistance to host defenses [12,64]. Erythrocyte hemolysis experiments showed that STs exhibited variable hemolytic capacities. In particular, the hemolytic activity of ST59 isolates varied and was significantly more robust than that of the ST398 and SST isolates. These findings are consistent with prior research showing a remarkably stronger hemolytic activity of ST59 than the ST398 isolates [65]. Regarding desiccation tolerance, an attribute linked to environmental persistence and capsule production [66], the clinical isolates showed similar resilience, with the SST strains having the lowest tolerance.

Our investigation into the covariation of virulence phenotypes revealed direct correlations between biofilm-related parameters, including early adhesion, biomass, cell metabolic activity in biofilm, and biofilm viable cells. This co-regulation emphasizes the complex nature of biofilm development and supports the idea that interventions targeting multiple stages of biofilm formation may be necessary to effectively control biofilm-related colonization of the skin of people with AD.

Based on 73 ARG/VF genes and eight phenotypic factors,

phylogenetic analysis yielded distinct clusters that did not correspond with virulence phenotypes. The correlation coefficient between phylogenetic and phenotypic distances indicates a lack of direct linkage between genetic proximity and phenotypic expression [67]. These results suggest that phenotypic traits are not dependent on specific bacterial subtypes or their phylogenetic relationships [67]. The observation that phylogenetic variability did not align with phenotypic variability indicates that other factors, potentially including the specific microenvironment of the skin in people with AD or non-structural genetic modifications (e.g., promoter activity, translation efficiency, mRNA stability) [68], might play significant roles. Genetic analysis of *S. aureus* populations from people with AD has revealed a heterogeneous genotype distribution that does not fully elucidate the mechanism behind the association of atopic skin with *S. aureus* [19,69]. The lack of correlation between *S. aureus* phylogeny and phenotypic clustering may suggest adaptive evolution where diverse genetic backgrounds lead to similar phenotypic adaptations beneficial for survival in AD lesions. This adaptive convergence could result from selective pressures within the AD skin microenvironment, such as inflammatory mediators, antimicrobial peptides, and nutrient availability, necessitating specific virulence attributes for colonization and persistence [62,70]. The common phenotypic traits, such as adhesion and biofilm formation, could thus be manifestations of convergent evolutionary strategies optimized for maintaining colonization and evading host defenses within the AD niche [62].

The findings highlight the complexity of virulence expression in AD-associated *S. aureus* and the limitations of relying solely on genomic data to predict phenotypic outcomes. It underscores the necessity of considering environmental and non-genetic factors in understanding the behavior of these pathogens. This study supports the broader application of integrated approaches in developing strategies for AD management, emphasizing the role of genetic and non-genetic influences in shaping pathogen behavior.

Despite the comprehensive analysis presented, this study has several limitations. Firstly, the sample size, although adequate for a pilot study, may only partially represent the diversity within people with AD or *S. aureus* strains, potentially limiting the generalizability of the findings. Secondly, the *in vitro* phenotypic assays may not fully recapitulate the complex *in vivo* environment of the skin [71]. It is important to acknowledge that *in vitro* systems, while valuable for elucidating mechanistic insights, lack the full complexity of the skin's microenvironment, which includes the dynamic interplay between the microbiome, immune responses, and environmental factors such as moisture and pH. For example, biofilm formation or the expression of bacterial virulence factors such as enterotoxins can be highly dependent on environmental conditions, which differ substantially between *in vitro* settings and the host's natural inflammatory environment. *In vitro* assays, with their artificial nutrient availability and lack of host immune pressures, may not induce the same gene expression patterns seen *in vivo*. Additionally, skin barrier function, often impaired in AD, and variations in immune cell recruitment play critical roles in modulating microbial colonization and infection. Thus, the observed phenotypes may significantly differ under *in vivo* conditions. Regardless of these limitations, the study offers valuable insights into the skin microbiome's role in AD and the complex interplay between the genotype and phenotype of *S. aureus*. The genetic variability and common virulence traits point to potential convergent evolution, favoring survival in the AD skin microenvironment. Future research should address these limitations and validate the findings in larger, more diverse cohorts, with longitudinal designs to explore the temporal dynamics of the microbiome and *S. aureus* populations in AD.

5. Conclusion

This study underscores the disrupted skin barrier and altered microbiome in AD, marked by increased prevalence of *S. aureus* and

S. lugdunensis. Network analysis revealed higher bacterial stability in HS, while AD-affected skin exhibited competitive interactions between *S. aureus* and the bacterial population, likely contributing to its persistence and dominance. WGS showed genetic diversity among *S. aureus* isolates but phenotypic convergence in traits like adhesion and biofilm formation, suggesting adaptive evolution. These findings highlight the need for integrated approaches considering genetic and non-genetic factors in AD management and call for further research to validate these insights in larger cohorts.

Data availability

The data for this study have been deposited in the European Nucleotide Archive (ENA) at EMBL-EBI under accession number PRJEB75009 (https://www.ebi.ac.uk/ena/browser/view/PRJEB75009).

Conflicts of interest

The authors declare that they have no known competing financial interests or personal relationships that could have appeared to influence the work reported in this paper.

CRediT authorship contribution statement

Francesca Sivori: Writing – review & editing, Visualization, Validation, Methodology, Investigation, Formal analysis, Data curation, Conceptualization. **Ilaria Cavallo:** Writing – review & editing, Validation, Methodology, Investigation, Formal analysis, Data curation, Conceptualization. **Mauro Truglio:** Writing – review & editing, Visualization, Validation, Software, Methodology, Investigation, Formal analysis, Data curation. **Flavio De Maio:** Writing – review & editing, Visualization, Software, Methodology, Formal analysis, Data curation. **Maurizio Sanguinetti:** Writing – review & editing, Validation, Supervision, Methodology, Data curation. **Giorgia Fabrizio:** Writing – review & editing, Methodology, Investigation, Formal analysis, Data curation. **Valerio Licursi:** Writing – review & editing, Validation, Software, Methodology, Formal analysis, Data curation. **Massimo Francalancia:** Validation, Methodology, Investigation, Formal analysis, Data curation. **Fulvia Fraticelli:** Methodology, Investigation, Formal analysis, Data curation. **Ilenia La Greca:** Methodology, Formal analysis, Data curation. **Federica Lucantoni:** Validation, Methodology, Formal analysis, Data curation. **Emanuela Camera:** Writing – review & editing, Methodology, Investigation, Formal analysis, Data curation. **Maria Mariano:** Validation, Investigation, Formal analysis, Data curation, Conceptualization. **Fiorentina Ascenzioni:** Writing – original draft, Validation, Supervision, Investigation, Formal analysis, Data curation. **Antonio Cristaudo:** Writing – review & editing, Methodology, Investigation, Funding acquisition, Formal analysis, Data curation, Conceptualization. **Fulvia Pimpinelli:** Writing – review & editing, Validation, Project administration, Methodology, Investigation, Formal analysis, Data curation, Conceptualization. **Enea Gino Di Domenico:** Writing – original draft, Supervision, Project administration, Methodology, Investigation, Funding acquisition, Formal analysis, Data curation, Conceptualization.

Declaration of competing interest

The authors declare that they have no known competing financial interests or personal relationships that could have appeared to influence the work reported in this paper.

Data availability

Data will be made available on request.

Appendix A. Supplementary data

Supplementary data to this article can be found online at https://doi.org/10.1016/j.bioflm.2024.100222.

References

[1] Weidinger S, Beck LA, Bieber T, Kabashima K, Irvine AD. Atopic dermatitis. Nat Rev Dis Prim 2018;4:1.

[2] Williams MR, Gallo RL. The role of the skin microbiome in atopic dermatitis. Curr Allergy Asthma Rep 2015;15:65.

[3] Paller AS, Kong HH, Seed P, Naik S, Scharschmidt TC, Gallo RL, Luger T, Irvine AD. The microbiome in patients with atopic dermatitis. J Allergy Clin Immunol 2019; 143:26–35.

[4] Byrd AL, Deming C, Cassidy SKB, Harrison OJ, Ng W-I, Conlan S, , NISC Comparative Sequencing Program, Belkaid Y, Segre JA, Kong HH. *Staphylococcus aureus* and *Staphylococcus epidermidis* strain diversity underlying pediatric atopic dermatitis. Sci Transl Med 2017;9:eaal4651.

[5] Nakatsuji T, Chen TH, Narala S, Chun KA, Two AM, Yun T, Shafiq F, Kotol PF, Bouslimani A, Melnik AV, Latif H, Kim J-N, Lockhart A, Artis K, David G, Taylor P, Streib J, Dorrestein PC, Grier A, Gill SR, Zengler K, Hata TR, Leung DYM, Gallo RL. Antimicrobials from human skin commensal bacteria protect against *Staphylococcus aureus* and are deficient in atopic dermatitis. Sci Transl Med 2017;9: eaah4680.

[6] Di Domenico EG, Cavallo I, Capitanio B, Ascenzioni F, Pimpinelli F, Morrone A, Ensoli F. Staphylococcus aureus and the cutaneous microbiota biofilms in the pathogenesis of atopic dermatitis. Microorganisms 2019;7:301.

[7] Kong HH, Oh J, Deming C, Conlan S, Grice EA, Beatson MA, Nomicos E, Polley EC, Komarow HD, , NISC Comparative Sequence Program, Murray PR, Turner ML, Segre JA. Temporal shifts in the skin microbiome associated with disease flares and treatment in children with atopic dermatitis. Genome Res 2012;22:850–9.

[8] Gallo RL, Horswill AR. Staphylococcus aureus: the bug behind the itch in atopic dermatitis. J Invest Dermatol 2024;144:950–3.

[9] Kim J, Kim BE, Berdyshev E, Bronova I, Bin L, Bae J, Kim S, Kim H, Lee UH, Kim MS, Kim H, Lee J, Hall CF, Hui-Beckman J, Chang Y, Bronoff AS, Hwang D, Lee H, Goleva E, Ahn K, Leung DYM. *Staphylococcus aureus* causes aberrant epidermal lipid composition and skin barrier dysfunction. Allergy 2023;78: 1292–306.

[10] Baurecht H, Rühlemann MC, Rodríguez E, Thielking F, Harder I, Erkens A-S, Stölzl D, Ellinghaus E, Hotze M, Lieb W, Wang S, Heinsen-Groth F-A, Franke A, Weidinger S. Epidermal lipid composition, barrier integrity, and eczematous inflammation are associated with skin microbiome configuration. J Allergy Clin Immunol 2018;141:1668–1676.e16.

[11] Kim J, Kim BE, Berdyshev E, Bronova I, Bin L, Bae J, Kim S, Kim H, Lee UH, Kim MS, Kim H, Lee J, Hall CF, Hui-Beckman J, Chang Y, Bronoff AS, Hwang D, Lee H, Goleva E, Ahn K, Leung DYM. *Staphylococcus aureus* causes aberrant epidermal lipid composition and skin barrier dysfunction. Allergy 2023;78: 1292–306.

[12] Di Domenico EG, Cavallo I, Bordignon V, Prignano G, Sperduti I, Gurtner A, Trento E, Toma L, Pimpinelli F, Capitanio B, Ensoli F. Inflammatory cytokines and biofilm production sustain Staphylococcus aureus outgrowth and persistence: a pivotal interplay in the pathogenesis of Atopic Dermatitis. Sci Rep 2018;8:9573.

[13] Allen HB, Vaze ND, Choi C, Hailu T, Tulbert BH, Cusack CA, Joshi SG. The presence and impact of biofilm-producing staphylococci in atopic dermatitis. JAMA Dermatol 2014;150:260.

[14] Foster TJ. The MSCRAMM family of cell-wall-anchored surface proteins of gram-positive cocci. Trends Microbiol 2019;27:927–41.

[15] Karygianni L, Ren Z, Koo H, Thurnheer T. Biofilm matrixome: extracellular components in structured microbial communities. Trends Microbiol 2020;28: 668–81.

[16] Tong SYC, Davis JS, Eichenberger E, Holland TL, Fowler VG. Staphylococcus aureus infections: epidemiology, pathophysiology, clinical manifestations, and management. Clin Microbiol Rev 2015;28:603–61.

[17] Harkins CP, Pettigrew KA, Oravcová K, Gardner J, Hearn RMR, Rice D, Mather AE, Parkhill J, Brown SJ, Proby CM, Holden MTG. The microevolution and epidemiology of Staphylococcus aureus colonization during atopic Eczema disease flare. J Invest Dermatol 2018;138:336–43.

[18] Key FM, Khadka VD, Romo-González C, Blake KJ, Deng L, Lynn TC, Lee JC, Chiu IM, García-Romero MT, Lieberman TD. On-person adaptive evolution of Staphylococcus aureus during treatment for atopic dermatitis. Cell Host Microbe 2023;31:593–603.e7.

[19] Ogonowska P, Gilaberte Y, Barańska-Rybak W, Nakonieczna J. Colonization with Staphylococcus aureus in atopic dermatitis patients: attempts to reveal the unknown. Front Microbiol 2021;11:567090.

[20] Cristaudo A, Pigliacelli F, Sperati F, Orsini D, Cameli N, Morrone A, Mariano M. Instrumental evaluation of skin barrier function and clinical outcomes during dupilumab treatment for atopic dermatitis: an observational study. Skin Res Technol 2021;27:810–3.

[21] Di Domenico EG, Toma L, Prignano G, Pelagalli L, Police A, Cavallotti C, Torelli R, Sanguinetti M, Ensoli F. Misidentification of Streptococcus uberis as a human pathogen: a case report and literature review. Int J Infect Dis 2015;33:79–81.

[22] Conte AL, Brunetti F, Marazzato M, Longhi C, Maurizi L, Raponi G, Palamara AT, Grassi S, Conte MP. Atopic dermatitis-derived Staphylococcus aureus strains: what makes them special in the interplay with the host. Front Cell Infect Microbiol 2023; 13:1194254.

[23] Cavallo I, Sivori F, Truglio M, De Maio F, Lucantoni F, Cardinali G, Pontone M, Bernardi T, Sanguinetti M, Capitanio B, Cristaudo A, Ascenzioni F, Morrone A, Pimpinelli F, Di Domenico EG. Skin dysbiosis and Cutibacterium acnes biofilm in inflammatory acne lesions of adolescents. Sci Rep 2022;12:21104.

[24] Segata N, Izard J, Waldron L, Gevers D, Miropolsky L, Garrett WS, Huttenhower C. Metagenomic biomarker discovery and explanation. Genome Biol 2011;12:R60.

[25] Truglio M, Sivori F, Cavallo I, Abril E, Licursi V, Fabrizio G, Cardinali G, Pignatti M, Toma L, Valensise F, Cristaudo A, Pimpinelli F, Di Domenico EG. Modulating the skin mycobiome-bacteriome and treating seborrheic dermatitis with a probiotic-enriched oily suspension. Sci Rep 2024;14:2722.

[26] Chen S, Zhou Y, Chen Y, Gu J. fastp: an ultra-fast all-in-one FASTQ preprocessor. Bioinformatics 2018;34:i884–90.

[27] Bankevich A, Nurk S, Antipov D, Gurevich AA, Dvorkin M, Kulikov AS, Lesin VM, Nikolenko SI, Pham S, Prjibelski AD, Pyshkin AV, Sirotkin AV, Vyahhi N, Tesler G, Alekseyev MA, Pevzner PA. SPAdes: a new genome assembly algorithm and its applications to single-cell sequencing. J Comput Biol 2012;19:455–77.

[28] Page AJ, Cummins CA, Hunt M, Wong VK, Reuter S, Holden MTG, Fookes M, Falush D, Keane JA, Parkhill J. Roary: rapid large-scale prokaryote pan genome analysis. Bioinformatics 2015;31:3691–3.

[29] Alcock BP, Huynh W, Chalil R, Smith KW, Raphenya AR, Wlodarski MA, Edalatmand A, Petkau A, Syed SA, Tsang KK, Baker SJC, Dave M, McCarthy MC, Mukiri KM, Nasir JA, Golbon B, Imtiaz H, Jiang X, Kaur K, Kwong M, Liang ZC, Niu KC, Shan P, Yang JYJ, Gray KL, Hoad GR, Jia B, Bhando T, Carfrae LA, Farha MA, French S, Gordzevich R, Rachwalski K, Tu MM, Bordeleau E, Dooley D, Griffiths E, Zubyk HL, Brown ED, Maguire F, Beiko RG, Hsiao WWL, Brinkman FSL, Van Domselaar G, McArthur AG. Card 2023: expanded curation, support for machine learning, and resistome prediction at the Comprehensive Antibiotic Resistance Database. Nucleic Acids Res 2023;51:D690–9.

[30] Chen L, Zheng D, Liu B, Yang J, Jin Q. Vfdb 2016: hierarchical and refined dataset for big data analysis—10 years on. Nucleic Acids Res 2016;44:D694–7.

[31] Di Domenico EG, Marchesi F, Cavallo I, Toma L, Sivori F, Papa E, Spadea A, Cafarella G, Terrenato I, Prignano G, Pimpinelli F, Mastrofrancesco A, D'Agosto G, Trento E, Morrone A, Mengarelli A, Ensoli F. The impact of bacterial biofilms on end-organ disease and mortality in patients with hematologic malignancies developing a bloodstream infection. Microbiol Spectr 2021;9:e0055021.

[32] Sivori F, Cavallo I, Kovacs D, Guembe M, Sperduti I, Truglio M, Pasqua M, Prignano G, Mastrofrancesco A, Toma L, Pimpinelli F, Morrone A, Ensoli F, Di Domenico EG. Role of extracellular DNA in dalbavancin activity against methicillin-resistant Staphylococcus aureus (MRSA) biofilms in patients with skin and soft tissue infections. Microbiol Spectr 2022;10:e0035122.

[33] Surre J, Canard I, Bourne-Branchu P, Courbiere E, Franceschi C, Chatellier S, Van Belkum A, Ramjeet M. Enhanced detection of carbapenemase-producing Enterobacteriaceae by an optimized phenol red assay. Diagn Microbiol Infect Dis 2018;90:11–7.

[34] Feng J, Sun D, Wang L, Li X, Guan J, Wei L, Yue D, Wang X, Zhao Y, Yang H, Song W, Wang B. Biochanin A as an α-hemolysin inhibitor for combating methicillin-resistant Staphylococcus aureus infection. World J Microbiol Biotechnol 2022;38:6.

[35] Greene C, Vadlamudi G, Newton D, Foxman B, Xi C. The influence of biofilm formation and multidrug resistance on environmental survival of clinical and environmental isolates of Acinetobacter baumannii. Am J Infect Control 2016;44: e65–71.

[36] Fueyo JM, Mendoza MC, Rodicio MR, Muñiz J, Alvarez MA, Martín MC. Cytotoxin and pyrogenic toxin superantigen gene profiles of Staphylococcus aureus associated with subclinical mastitis in dairy cows and relationships with macrorestriction genomic profiles. J Clin Microbiol 2005;43:1278–84.

[37] Makarova O, Johnston P, Walther B, Rolff J, Roesler U. Complete genome sequence of the disinfectant susceptibility testing reference strain Staphylococcus aureus subsp. *aureus* ATCC 6538. Genome Announc 2017;5:e0029317.

[38] Leshem YA, Hajar T, Hanifin JM, Simpson EL. What the Eczema Area and Severity Index score tells us about the severity of atopic dermatitis: an interpretability study. Br J Dermatol 2015;172:1353–7.

[39] Nakatsuji T, Hata TR, Tong Y, Cheng JY, Shafiq F, Butcher AM, Salem SS, Brinton SL, Rudman Spergel AK, Johnson K, Jepson B, Calatroni A, David G, Ramirez-Gama M, Taylor P, Leung DYM, Gallo RL. Development of a human skin commensal microbe for bacteriotherapy of atopic dermatitis and use in a phase 1 randomized clinical trial. Nat Med 2021;27:700–9.

[40] Danby SG, Al-Enezi T, Sultan A, Chittock J, Kennedy K, Cork MJ. The effect of aqueous cream BP on the skin barrier in volunteers with a previous history of atopic dermatitis: effect of aqueous cream BP on the skin barrier. Br J Dermatol 2011;165:329–34.

[41] Fluhr JW, Feingold KR, Elias PM. Transepidermal water loss reflects permeability barrier status: validation in human and rodent *in vivo* and *ex vivo* models. Exp Dermatol 2006;15:483–92.

[42] Elias PM, Schmuth M. Abnormal skin barrier in the etiopathogenesis of atopic dermatitis. Curr Allergy Asthma Rep 2009;9:265–72.

[43] Ye L, Wang Z, Li Z, Lv C, Man M-Q. Validation of GPS kin Barrier ® for assessing epidermal permeability barrier function and stratum corneum hydration in humans. Skin Res Technol 2019;25:25–9.

[44] Bjerre RD, Holm JB, Palleja A, Sølberg J, Skov L, Johansen JD. Skin dysbiosis in the microbiome of atopic dermatitis is site-specific and involves bacteria, fungus and virus. BMC Microbiol 2021;21:256.

[45] Costello EK, Lauber CL, Hamady M, Fierer N, Gordon JI, Knight R. Bacterial community variation in human body habitats across space and time. Science 2009; 326:1694–7.

[46] SanMiguel A, Grice EA. Interactions between host factors and the skin microbiome. Cell Mol Life Sci 2015;72:1499–515.

[47] McLaughlin J, Watterson S, Layton AM, Bjourson AJ, Barnard E, McDowell A. Propionibacterium acnes and acne vulgaris: new insights from the integration of population genetic, multi-omic, biochemical and host-microbe studies. Microorganisms 2019;7:128.

[48] Rozas M, Hart De Ruijter A, Fabrega MJ, Zorgani A, Guell M, Paetzold B, Brillet F. From dysbiosis to healthy skin: major Contributions of Cutibacterium acnes to skin homeostasis. Microorganisms 2021;9:628.

[49] Dekio I, Asahina A, Shah HN. Unravelling the eco-specificity and pathophysiological properties of Cutibacterium species in the light of recent taxonomic changes. Anaerobe 2021;71:102411.

[50] Leung MHY, Tong X, Shen Z, Du S, Bastien P, Appenzeller BMR, Betts RJ, Mezzache S, Bourokba N, Cavusoglu N, Aguilar L, Misra N, Clavaud C, Lee PKH. Skin microbiome differentiates into distinct cutotypes with unique metabolic functions upon exposure to polycyclic aromatic hydrocarbons. Microbiome 2023; 11:124.

[51] Harel N, Ogen-Shtern N, Reshef L, Biran D, Ron EZ, Gophna U. Skin microbiome bacteria enriched following long sun exposure can reduce oxidative damage. Res Microbiol 2023;174:104138.

[52] Edslev SM, Olesen CM, Nørreslet LB, Ingham AC, Iversen S, Lilje B, Clausen M-L, Jensen JS, Stegger M, Agner T, Andersen PS. Staphylococcal communities on skin are associated with atopic dermatitis and disease severity. Microorganisms 2021;9: 432.

[53] Nakatsuji T, Gallo RL. The role of the skin microbiome in atopic dermatitis. Ann Allergy Asthma Immunol 2019;122:263–9.

[54] Williams MR, Cau L, Wang Y, Kaul D, Sanford JA, Zaramela LS, Khalil S, Butcher AM, Zengler K, Horswill AR, Dupont CL, Hovnanian A, Gallo RL. Interplay of staphylococcal and host proteases promotes skin barrier disruption in netherton syndrome. Cell Rep 2020;30:2923–2933.e7.

[55] Gomes Pw P, Mannochio-Russo H, Mao J, Zhao HN, Ancira J, Tipton CD, Dorrestein PC, Li M. Co-occurrence network analysis reveals the alterations of the skin microbiome and metabolome in adults with mild to moderate atopic dermatitis. mSystems 2024;9:e0111923.

[56] Wang L, Yu T, Zhu Y, Luo Y, Dong F, Lin X, Zhao W, He Z, Hu S, Dong Z. Amplicon-based sequencing and co-occurrence network analysis reveals notable differences of microbial community structure in healthy and dandruff scalps. BMC Genom 2022;23:312.

[57] Coyte KZ, Schluter J, Foster KR. The ecology of the microbiome: networks, competition, and stability. Science 2015;350:663–6.

[58] Becker K, Ballhausen B, Kahl BC, Köck R. The clinical impact of livestock-associated methicillin-resistant Staphylococcus aureus of the clonal complex 398 for humans. Vet Microbiol 2017;200:33–8.

[59] Jian Y, Zhao L, Zhao N, Lv H-Y, Liu Y, He L, Liu Q, Li M. Increasing prevalence of hypervirulent ST5 methicillin susceptible *Staphylococcus aureus* subtype poses a serious clinical threat. Emerg Microb Infect 2021;10:109–22.

[60] Gu J, Shen S, Xiong M, Zhao J, Tian H, Xiao X, Li Y. ST7 becomes one of the most common Staphylococcus aureus clones after the COVID-19 epidemic in the city of wuhan, China. Infect Drug Resist 2023;16:843–52.

[61] Zhao H, Wu X, Wang B, Shen L, Rao L, Wang X, Zhang J, Xiao Y, Xu Y, Yu J, Guo Y, Zhou Y, Wan B, Wu C, Chen L, Yu F. Phenotypic and genomic analysis of the hypervirulent ST22 methicillin-resistant *Staphylococcus aureus* in China. mSystems 2023;8:e0124222.

[62] Blicharz L, Szymanek-Majchrzak K, Młynarczyk G, Czuwara J, Waśkiel-Burnat A, Goldust M, Samochocki Z, Rudnicka L. Multilocus-sequence typing reveals clonality of *Staphylococcus aureus* in atopic dermatitis. Clin Exp Dermatol 2023;48: 1341–6.

[63] Stepanović S, Vuković D, Dakić I, Savić B, Švabić-Vlahović M. A modified microtiter-plate test for quantification of staphylococcal biofilm formation. J Microbiol Methods 2000;40:175–9.

[64] O'Gara JP. *Ica* and beyond: biofilm mechanisms and regulation in *Staphylococcus epidermidis* and *Staphylococcus aureus*. FEMS Microbiol Lett 2007;270:179–88.

[65] Liu L, Peng H, Zhang N, Li M, Chen Z, Shang W, Hu Z, Wang Y, Yang Y, Wang D, Hu Q, Rao X. Genomic epidemiology and phenotypic characterization of Staphylococcus aureus from a tertiary hospital in tianjin municipality, northern China. Microbiol Spectr 2023;11:e04209–22.

[66] Wang H, Shen J, Ma K, Zhu C, Fang M, Hou X, Zhang S, Wang W, Xue T. Transcriptome analysis revealed the role of capsular polysaccharides in desiccation tolerance of foodborne Staphylococcus aureus. Food Res Int 2022;159:111602.

[67] Scheffler RJ, Bratton BP, Gitai Z. Pseudomonas aeruginosa clinical blood isolates display significant phenotypic variability. PLoS One 2022;17:e0270576.

[68] Kruczek C, Kottapalli KR, Dissanaike S, Dzvova N, Griswold JA, Colmer-Hamood JA, Hamood AN. Major transcriptome changes accompany the growth of Pseudomonas aeruginosa in blood from patients with severe thermal injuries. PLoS One 2016;11:e0149229.

[69] Ogonowska P, Szymczak K, Empel J, Urbaś M, Woźniak-Pawlikowska A, Barańska-Rybak W, Świetlik D, Nakonieczna J. Staphylococcus aureus from atopic dermatitis patients: its genetic structure and susceptibility to phototreatment. Microbiol Spectr 2023;11:e0459822.

[70] Wong Fok Lung T, Chan LC, Prince A, Yeaman MR, Archer NK, Aman MJ, Proctor RA. Staphylococcus aureus adaptive evolution: recent insights on how immune evasion, immunometabolic subversion and host genetics impact vaccine development. Front Cell Infect Microbiol 2022;12:1060810.

[71] Costa FG, Mills KB, Crosby HA, Horswill AR. The *Staphylococcus aureus* regulatory program in a human skin-like environment. mBio 2024;e00453–24.